FUDMA Journal of Sciences (FJS)
ISSN online: 2616-1370
ISSN print: 2645 - 2944
Vol. 10 No. 10, May, 2026, pp 125 – 136
DOI: https://doi.org/10.33003/fjs-2026-1010-5488

Numerical Investigation of a Fractional-Order Measles Model via the Generalized Adams–Bashforth–Moulton Technique

[1]David Omale, [*1]Jeremiah Amos, William Atokolo, [1,2]Enejoh Jalija, Emmanuel Abah, [3]Danladi Egbunu, [4]Simon Adukwu Iyaji

[1]Department of Mathematical Sciences, Prince Abubakar Audu University, Anyigba, Kogi State, Nigeria.
[2]Department of Mathematics and statistics, The Federal Polytechnic Idah, Kogi State, Nigeria.
[3]Department of Civil Engineering, The Federal Polytechnic Idah, Kogi State, Nigeria.
[4]Department of Economics, Prince Abubakar Audu University, Anyigba, Kogi State, Nigeria.

*Corresponding authors' email: amosjeremiah1997@gmail.com

ABSTRACT

In this research, the transmission dynamics of Measles are investigated by adopting a fractional-order mathematical model to investigate the impact of vaccination, treatment and contacts on the transmission of the disease. The model is well-posed, containing solutions and uniqueness, in fractional order sense. Stability analysis of the model is carried out to investigate the disease dynamics, including the determination of the basic reproduction number. The results show that treating infected individuals more often plays an important role in keeping the basic reproduction number below one and thus actually supports the control of the disease, while the higher the contact rate, the more the disease can be transmitted and persistent in the population. In addition, simulation analyses show that transmission related parameters are favorable for disease transmission, while treatment and vaccination related parameters are unfavorable for spread and contribute to a decrease of the disease burden. The fractional Adams–Bashforth–Moulton numerical scheme is used to study the dynamics of the population compartments under the different rates of treatment and contact. The results highlight that treatment and large scale vaccination of susceptible people is key to reducing the burden of Measles. Finally, the study shows that the use of integrated control measures, such as treatment expansion, vaccination coverage and reducing transmission pathways can be used effectively to control and potentially eradicate Measles in the population.

Keywords: Measles, Fractional, Adam-Bashforth-Moulton, Transmission, Control, strategies

INTRODUCTION

Measles is a highly contagious viral illness resulting from infection of the body with the Morbillivirus. It primarily affects children, but people of all ages who are not immunized can get sick. Measles invades the respiratory tract, then spreads throughout the body. The common symptoms are fever, cough, runny nose, red and watery eyes, sore throat and a characteristic rash that starts on the face and then spreads to other parts of the body. Complications of measles can be serious, such as pneumonia, encephalitis, diarrhea, blindness, and death, particularly for those with compromised immune systems and malnutrition. Spreads person to person via respiratory droplets generated by an infected person who coughs or sneezes. Although outbreaks still occur in many parts of the world where vaccination coverage is inadequate, vaccination is the most effective way of preventing and controlling the disease.

Even after many decades of successful vaccines being available, measles has still remained a major public health problem worldwide. Prior to 1963 when the vaccine was introduced, the measles was a major epidemic that occurred every 2 to 3 years, killing millions of people around the world. Measles is one of the top ten causes of child morbidity and mortality in Nigeria. It has been present in the country for many years and has caused outbreaks of the disease in various parts of the country. The disease has been persisting due to inadequate immunization coverage, poor access to health care facilities, malnutrition and population movement. Multiple vaccination campaigns have been conducted, but outbreaks are still occurring, especially among young children (less than 5 years of age). Health officials' reports indicate that Nigeria is still one of the nations with the highest number of cases of measles in Africa, which remains a critical public health issue for both health practitioners and policymakers.

With the growing burden and complexity of infectious diseases, there has been a growing need to develop mathematical models to understand the dynamics of the disease and to assess strategies for disease intervention. Due to its ability to gain insight into the transmission process and make predictions of disease trends, mathematical modeling is an essential tool in epidemiology. Classical integer-order models have received extensive use in the study of the dynamics of infectious diseases, but memory and hereditary effects that are inherent in biological systems cannot be accounted for. As a result, researchers have turned their focus to fractional calculus, due to the ability of fractional derivatives to model memory effects and give more realistic models of disease progression.

Fractional-order models are of great interest due to their flexibility and applicability in the description of complex biological systems. The fractional-order models describe the whole history of the system, unlike integer-order models, which describe only the local behavior of the system. Various singular kernel derivatives have been used in the modelling of epidemics, for instance, the Riemann–Liouville derivative and the Caputo derivative, and also non-singular kernel derivatives have received attention for the possibility of removing the singularities and giving more accurate descriptions of biological phenomena, such as the Caputo–Fabrizio derivative and the Atangana–Baleanu derivative.

Only a few researchers have used fractional calculus to study infectious diseases. In a paper of Atokolo et al. (2022) using a fractional-order approach to the control of Zika virus infection with the Laplace Adomian Decomposition Method, the authors showed that the results converge to exact

solutions. Yunus et al. (2023) studied the propagation of COVID-19 in Nigeria using the Caputo fractional derivative and found that treatment and vaccination were essential in improving the recovery process.

Omede et al. (2024) developed a fractional-order model to represent soil-transmitted helminth infections, showing that this approach yields more accurate and adaptable solutions than traditional integer-order models. Meanwhile, Amos et al. (2024) proposed a fractional-order framework for hepatitis C transmission, employing the Adams–Bashforth–Moulton technique for numerical simulations. Their findings indicated that reducing contact rates and expanding treatment coverage both play crucial roles in curtailing the spread of the disease.

Ahmed et al. (2021) examined the simultaneous transmission dynamics of HIV and COVID-19 using the Atangana–Baleanu fractional derivative, concluding that this mathematical approach effectively captures the complexities of disease spread. Similarly, Omame et al. (2022) investigated a fractional-order co-infection model for hepatitis B virus (HBV) and COVID-19, also employing the Atangana–Baleanu derivative, and determined that preventive measures play a critical role in managing the outbreak.

Acheneje et al. (2024) developed a fractional-order framework to model the co-infection dynamics of COVID-19 and monkeypox, using the Laplace Adomian Decomposition Method to generate numerical approximations aligned with empirical data. Their findings indicated that expanding treatment access contributes to a reduction in disease incidence. In a related review, Smith et al. (2023) synthesized existing mathematical models addressing hepatitis C and COVID-19 co-infection, advocating for further exploration using advanced mathematical techniques. Responding to this call, Atokolo et al. (2023) put forward a vector-borne disease model that incorporates both vertical transmission and preventive strategies, reinforcing the value of mathematical modeling in understanding disease propagation.

In the last years, researchers have been applying the mathematics of fractional calculus to the study of the dynamics of measles. Fractional-order measles models have been demonstrated to be more realistic models of disease transmission due to their ability of incorporating memory effects. The flexibility and non-local property of fractional derivatives make them appropriate model for epidemiological systems more than classical derivatives. Further, the memory property of fractional order models can be used to describe biological processes with higher accuracy, which could help in enhancing the predictive capability of the models and in developing suitable disease control strategies.

The main advantages of fractional-order mathematical models stem from their inherent flexibility, non-local behavior, and memory effects. These characteristics allow fractional derivatives to offer a more realistic representation of biological systems compared to traditional integer-order derivatives. As a result, fractional differential equations have attracted considerable attention across diverse disciplines, including physics, engineering, epidemiology, and mathematics. The utility of fractional calculus in examining complex systems has been demonstrated by Amos et al. (2024) through work on fuzzy Volterra integral equations, and by Abah et al. (2024) via stability analyses of fractional differential equations.

Numerous analytical and numerical techniques have been employed to tackle infectious disease modeling, including the Laplace Adomian Decomposition Method, the Homotopy Perturbation Method, the Differential Transform Method, and the Adams–Bashforth–Moulton scheme. The fractional-order version of the Adams–Bashforth–Moulton method, in particular, has drawn widespread attention from scholars due to its reliability and computational efficiency in solving fractional differential equations. Furthermore, Lyapunov functions have proven to be a crucial instrument for analyzing the long-term behavior of equilibrium states in epidemiological systems and have consequently gained significant traction in the field.

Fractional-order models are very useful because they are more flexible and are more realistic in the description of the dynamics of the disease compared to classical models. Their storability of memory elements and hereditary property can reflect the complicated mechanism that occurs in the transmission of disease. For this reason the use of fractional differential equations in the modeling of infectious diseases has become more common among researchers, and is expected to continue to support the development of mathematical epidemiology in the future.

This study aims to formulate a fractional-order mathematical model for the transmission dynamics of measles, establish sufficient conditions for the existence and uniqueness of solutions to the mathematical model, investigate the stability properties of the equilibrium states of the model using appropriate analytical methods, obtain numerical solutions of the mathematical model by the fractional Adams–Bashforth–Moulton method, and make simulations to consider the effects of the important epidemiological parameters on the transmission dynamics of measles.

Analysis of the literature pointed out that there are only a few works that have studied measles dynamics from classical and fractional-order perspectives, but very little research has focused on the detailed existence, uniqueness and stability analysis of the fractional Adams–Bashforth–Moulton method for the study of measles transmission. This is the motivation for the present study.

Preliminaries

Definition 1

Let $f \in \Lambda^{\infty}(R)$, The left and right Caputo fractional derivatives of the function f are then defined as

$$ {}^{c}D_{t}^{\vartheta} f(t) = \left(t^{0}D_{t}^{-(n\vartheta)} \left(\frac{d}{dt}\right)^{n} f(t) \right),$$

$$ {}^{c}D_{t}^{\vartheta} f(t) = \frac{1}{\Gamma(n-\vartheta)} \int_{0}^{t} \left((t-\lambda)^{n-\vartheta-1} f^{n}(\lambda) \right) d\lambda, \quad (1)$$

Similarly

$$ {}_{T}^{c}D_{t}^{\vartheta} f(t) = \left({}_{t}D_{T}^{-(n-\vartheta)} \left(\frac{-d}{dt}\right)^{n} f(t) \right),$$

$$ {}_{T}^{c}D_{T}^{\vartheta} f(t) = \frac{(-1)^{n}}{\Gamma(n-\vartheta)} \int_{t}^{T} \left((\lambda-t)^{n-\vartheta-1} f^{n}(\lambda) \right) d\lambda,$$

Definition 2

The generalized Mittag-Leffler function $E_{\vartheta,\beta}(x)$ for $x \in R$ is given by:

$$E_{\vartheta,\beta}(x) = \sum_{n=0}^{\infty} \frac{x^n}{\Gamma(\vartheta n+\beta)}, \vartheta, \beta > 0 \quad (2)$$

which can be denoted as;

$$E_{\vartheta,\beta}(x) = xE_{\vartheta,\vartheta\frac{x-\mu}{\vartheta}+\beta(x)} + \frac{1}{\Gamma(\beta)} \quad (3)$$

$$E_{\vartheta,\beta}(x) = L\left[t^{\beta-1}E_{\vartheta,\beta(\pm\omega t^{\vartheta})}\right] = \frac{S^{\vartheta-\beta}}{S^{\vartheta}\pm\omega} \quad (4)$$

Proposition 1.1

Let $f \in \Lambda^{\infty}(R) \cap C(R)$ and $\vartheta \in R, n-1 < \vartheta < n$,

therefore, the conditions given below is satisfied:

$$1.\ {}_{t_o}^{c}D_t^{\vartheta} I^{\vartheta} f(t) = f(t), \quad (5)$$

$$2.\ I_{t_o}^{\vartheta} D_t^{\vartheta} f(t) = f(t) - \sum_{k=0}^{n-k} \frac{t^k}{k!} f^k(t_o). \quad (6)$$

Model Formulation

The total human population $N_h$is divided into six mutually exclusive compartments: susceptible S_h, vaccinated V_h, exposed E_h, infected I_h, treated infected T_h, and recovered R_h, such that,

$N_h = S_h + E_h + I_h + T_h + V_h + R_h$.

Individuals are recruited into the susceptible class at rate π. Susceptible individuals are vaccinated at rate ψ_1, or die naturally at rate μ_h. Vaccinated individuals lose vaccine-induced immunity and return to the susceptible class at rate ψ_2 and also experience natural death at rate μ_h.Exposed individuals progress to the infectious class at rate θ and die naturally at rate μ_h. Infected individuals receive treatment at rate ϕ, recover through treatment indirectly, die naturally at rate μ_h, and experience disease-induced death at rate δ. Treated infected individuals recover at rate σ, die naturally at rate μ_h, and experience reduced disease-induced death at rate αδ, where 0<α<10<1.Recovered individuals acquire immunity and die naturally at rate μ_h. Overall, the model incorporates the key parameters governing recruitment (π), vaccination ψ_1, waning immunity ψ_2, progression (θ), treatment (ϕ), recovery (σ), natural mortality (μ_h), disease-induced mortality (δ), and treatment effectiveness (α), allowing assessment of vaccination and treatment impacts on disease dynamics.

Model Flow Diagram

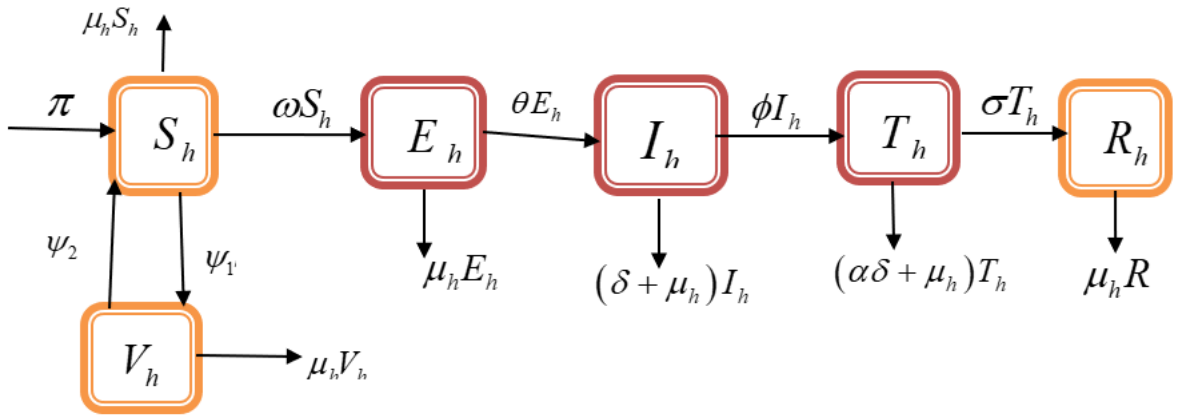

Figure 1: Measles Model Flow Diagram

Model Equation

$$\frac{dS_h}{dt} = \pi + \psi_2 V_h - \omega S_h - (\psi_1 + \mu_h)S_h,$$

$$\frac{dE_h}{dt} = \omega S_h - (\theta + \mu_h)E_h$$

$$\frac{dI_h}{dt} = \theta E_h - (\phi + \delta + \mu_h)I_h,$$

$$\frac{dT_h}{dt} = \phi I_h - (\sigma + \alpha\delta + \mu_h)T_h, \quad (7)$$

$$\frac{dV_h}{dt} = \psi_1 S_h - (\psi_2 + \mu_h)V_h,$$

$$\frac{dR_h}{dt} = \sigma T_h - \mu_h R_h.$$

Where, $\omega = \frac{(\varepsilon_1 I_h + \varepsilon_2 T_h)}{N_h}$

Table 1: Variable and Parameters Description

Variable	Description
S_h	Susceptible Human population to Measles
E_h	ExposedHuman population to Measles
I_h	Infected Human population with Measles
T_h	Human population on treatment
V_h	Vaccinated Humans against Measles
R_h	Recovered human population from Measles
Parameter Description	
Λ	Recruitment rate of humans
ε_1	Contact rate of susceptible and infected humans
ε_2	Contact rate of susceptible and humans on treatment.
ψ_1	Vaccination rate
ψ_2	Waning rate of vaccine.
δ	Disease induced death rate of infected humans
α	Modification parameter
μ_h	Natural death rate of humans
θ	Progression rate from Exposed to infected class
σ	Recovery due to treatment rate

Model Analysis

$$\begin{aligned}
\frac{dS_h}{dt} &= \pi + \psi_2 V_h - \frac{(\varepsilon_1 I_h + \varepsilon_2 T_h)}{N_h} S_h - (\psi_1 + \mu_h) S_h, \\
\frac{dE_h}{dt} &= \frac{(\varepsilon_1 I_h + \varepsilon_2 T_h)}{N_h} S_h - (\theta + \mu_h) E_h \\
\frac{dI_h}{dt} &= \theta E_h - (\phi + \delta + \mu_h) I_h, \\
\frac{dT_h}{dt} &= \phi I_h - (\sigma + \alpha\delta + \mu_h) T_h, \\
\frac{dV_h}{dt} &= \psi_1 S_h - (\psi_2 + \mu_h) V_h, \\
\frac{dR_h}{dt} &= \sigma T_h - \mu_h R_h.
\end{aligned} \tag{8}$$

Disease Free Equilibrium Point of Measles

Disease free equilibrium point is a point where there is no disease in the population

At DFE $S_h \neq 0, E_h = 0, I_h = 0, T_h = 0, V_h = 0, R_h = 0.$

$$\left(S_h^0, E_h^0, I_h^0, T_h^0, V_h^0, R_h^0\right) = \left(\frac{\pi(\psi_2+\mu_h)}{\mu_h(\psi_2+\psi_1+\mu_h)}, 0,0,0, \frac{\psi_1\pi}{\mu_h(\psi_2+\psi_1+\mu_h)}, 0\right). \tag{9}$$

Basic Reproduction Number of Measles

Basic Reproduction number R_0^M is the number of secondary cases caused by individual infected people. Next generation method $R_0^M = \rho F V^{-1}$ is used to compute R_0^M using F, a non negative matrix (other transition terms V) and finding the dominant Eigen value ρ.

$$F = \begin{pmatrix} 0 & \frac{\varepsilon_1(\psi_2+\mu_h)}{\psi_2+\psi_1+\mu_h} & \frac{\varepsilon_2(\psi_2+\mu_h)}{\psi_2+\psi_1+\mu_h} \\ 0 & 0 & 0 \\ 0 & 0 & 0 \end{pmatrix}, \text{ and} V = \begin{pmatrix} P_2 & 0 & 0 \\ -\theta & P_3 & 0 \\ 0 & -\phi & P_4 \end{pmatrix}, \tag{10}$$

$$V^{-1} = \begin{pmatrix} \frac{1}{P_2} & 0 & 0 \\ \frac{\theta}{P_2P_3} & \frac{1}{P_3} & 0 \\ \frac{\theta\phi}{P_2P_3P_4} & \frac{\phi}{P_3P_4} & \frac{1}{P_4} \end{pmatrix},$$

$$FV^{-1} = \begin{pmatrix} \frac{\varepsilon_1(\psi_2+\mu_h)\theta}{(\psi_2+\psi_1+\mu_h)P_2P_3} + \frac{\varepsilon_2(\psi_2+\mu_h)\theta\phi}{(\psi_2+\psi_1+\mu_h)P_2P_3P_4} & \frac{\varepsilon_1(\psi_2+\mu_h)}{(\psi_2+\psi_1+\mu_h)P_3} + \frac{\varepsilon_2(\psi_2+\mu_h)\phi}{(\psi_2+\psi_1+\mu_h)P_3P_4} & \frac{\varepsilon_2(\psi_2+\mu_h)}{(\psi_2+\psi_1+\mu_h)P_4} \\ 0 & 0 & 0 \\ 0 & 0 & 0 \end{pmatrix},$$

$$Eigenvalues = \begin{pmatrix} 0 \\ 0 \\ \frac{\theta(\phi\varepsilon_2\mu_h + \phi\varepsilon_2\psi_2 + P_4\varepsilon_1\mu_h + P_4\varepsilon_1\psi_2)}{(\psi_2+\psi_1+\mu_h)P_2P_3P_4} \end{pmatrix},$$

The basic reproduction number is:

$$R_0^M = \frac{\theta(\phi\varepsilon_2\mu_h+\phi\varepsilon_2\psi_2+P_4\varepsilon_1\mu_h+P_4\varepsilon_1\psi_2)}{(\psi_2+\psi_1+\mu_h)P_2P_3P_4}, \tag{11}$$

Where

$P_1 = (\psi_1 + \mu_h)$, $P_2 = (\theta + \mu_h)$, $P_3 = (\phi + \delta + \mu_h)$, $P_4 = (\sigma + \alpha\delta + \mu_h)$, $P_5 = (\psi_2 + \mu_h)$, $P_6 = \mu_h$.

$$R_0^M = \frac{\theta(\phi\varepsilon_2\mu_h + \phi\varepsilon_2\psi_2 + (\sigma+\alpha\delta+\mu_h)\varepsilon_1\mu_h + (\sigma+\alpha\delta+\mu_h)\varepsilon_1\psi_2)}{(\psi_2+\psi_1+\mu_h)(\theta+\mu_h)(\phi+\delta+\mu_h)(\sigma+\alpha\delta+\mu_h)}. \quad (12)$$

Endemic Equilibrium of Measles

Endemic Equilibrium signifies the permanent existence of Measles among human population.
At endemic equilibrium point ($S_h \neq 0, E_h \neq 0, I_h \neq 0, T_h \neq 0, V_h \neq 0, R_h \neq 0$).
We obtain the following endemic equilibrium points:

$$\begin{aligned}
S_h^{**} &= \frac{\pi P_5}{P_5(\omega + P_1) - \psi_1\psi_2},\\
E_h^{**} &= \frac{\omega\pi P_5}{P_2(P_5(\omega + P_1) - \psi_1\psi_2)},\\
I_h^{**} &= \frac{\theta\omega\pi P_5}{(P_5(\omega+P_1)-\psi_1\psi_2)P_3P_2},\\
T_h^{**} &= -\frac{\theta\omega\pi P_5\phi}{\big((-\omega - P_1)P_5 + \psi_1\psi_2\big)P_2P_4P_3},\\
V_h^{**} &= \frac{\pi\psi_1}{P_5\omega + P_5P_1 - \psi_1\psi_2},\\
R_h^{**} &= \frac{\sigma\theta\omega(V_h\psi_2 + \pi)\phi}{(\omega + P_1)P_2P_3P_4P_6}.
\end{aligned} \quad (13)$$

Substituting into the force of infection $\omega = \frac{(\varepsilon_1 I_h + \varepsilon_2 T_h)}{N_h}$.
We have:

$$\boldsymbol{Q_1\lambda + Q_2 = 0}$$

$$W_1 = (\phi\sigma\theta P_5 + \phi\theta P_5P_6 + \theta P_4P_5P_6 + P_3P_4P_5P_6),$$

$$W_2 = P_2\left(1 - \frac{\theta(\phi\varepsilon_2\mu_h + \phi\varepsilon_2\psi_2 + P_4\varepsilon_1\mu_h + P_4\varepsilon_1\psi_2)}{(\psi_2 + \psi_1 + \mu_h)P_2P_3P_4}\right),$$

$$\Rightarrow W_2 = P_2(1 - R_0^M). \quad (14)$$

This shows that the endemic equilibrium point of the model is stable and has a unique positive solution if $R_0^M > 1$.

Fractional-order Model Equation

$$\begin{aligned}
{}^cD_t^\vartheta S_h &= \pi + \psi_2V_h - \tfrac{(\varepsilon_1I_h+\varepsilon_2T_h)}{N_h}S_h - (\psi_1 + \mu_h)S_h,\\
{}^cD_t^\vartheta E_h &= \frac{(\varepsilon_1 I_h + \varepsilon_2 T_h)}{N_h}S_h - (\theta + \mu_h)E_h\\
{}^cD_t^\vartheta I_h &= \theta E_h - (\phi + \delta + \mu_h)I_h,\\
{}^cD_t^\vartheta T_h &= \phi I_h - (\sigma + \alpha\delta + \mu_h)T_h,\\
{}^cD_t^\vartheta V_h &= \psi_1S_h - (\psi_2 + \mu_h)V_h,\\
{}^cD_t^\vartheta R_h &= \sigma T_h - \mu_hR_h.
\end{aligned} \quad (15)$$

Subject to the initial conditions:
$S_h(0) = S_{h0}, E_h(0) = E_{h0}, I_h(0) = I_{h0}, T_h(0) = T_{h0}, V_h(0) = V_{h0}, R_h(0) = R_{h0}$.

Positivity of Model Solution

We considered the non-negativity of the initial values

$N_h(t) \leq \frac{\pi}{\mu_h}$ as $t \to \infty$

Secondly, $if\ limsup\, N_{h0}(t) \leq \frac{\pi}{\mu_h}$, then our model feasible domain is given by:

$$\Omega = \left\{(S_h, E_h, I_h, T_h, V_h, R_h) \subset R_+^6 : S_h + E_h + I_h + T_h + V_h + R_h \leq \frac{\pi}{\mu_h}\right\},$$

so that,
$\Omega = \Omega_h \subset R_+^6$,
hence Ω is positively invariant.
If $(S_{h0}, E_{h0}, I_{h0}, T_{h0}, V_{h0}, R_{h0})$ are non-negative, then the solution of model (7) will be non-negative for $t > 0$. From Eq. (7), selecting the first equation, we obtained:

$${}^cD_t^\vartheta S_h = \pi + \psi_2V_h - \frac{(\varepsilon_1 I_h + \varepsilon_2 T_h)}{N_h}S_h - (\psi_1 + \mu_h)S_h,$$

$${}^cD_t^\vartheta S_h + \frac{(\varepsilon_1 I_h + \varepsilon_2 T_h + \psi_1 + \mu_h)}{N_h}S_h = \pi + \psi_2V_h,$$

But $\pi + \psi_2V_h \geq 0$, then,

$${}^cD_t^\vartheta S_h + \frac{(\varepsilon_1 I_h + \varepsilon_2 T_h + \psi_1 + \mu_h)}{N_h}S_h \geq 0.$$

Applying the Laplace transform we obtained:

$$L\left[{}^cD_t^\vartheta S_h\right] + L\left[\frac{(\varepsilon_1 I_h + \varepsilon_2 T_h + \psi_1 + \mu_h)}{N_h}S_h\right] \geq 0,$$

$$S_h^{\vartheta} S_h(s) - S_h^{\vartheta-1} S_h(0) + \frac{(\varepsilon_1 I_h + \varepsilon_2 T_h + \psi_1 + \mu_h)}{N_h} S_h(s) \geq 0,$$

$$S_h(s) \geq \frac{S_h^{\vartheta-1}}{S_h^{\vartheta} + \frac{(\varepsilon_1 I_h + \varepsilon_2 T_h + \psi_1 + \mu_h)}{N_h}} S_h(0). \quad (16)$$

By taking the inverse Laplace transform, we obtained:

$$S_h(t) \geq E_{t\vartheta,1}\left(-\left(\frac{(\varepsilon_1 I_h + \varepsilon_2 T_h + \psi_1 + \mu_h)}{N_h}\right) t^{\vartheta}\right) S_{h0}. \quad (17)$$

Now, since the term on the right-hand side of Eq. (17) is positive, we conclude that $S_h \geq 0$ for $t \geq 0$. In the same way, we also have that $E_h \geq 0, I_h \geq 0, T_h \geq 0, V_h \geq 0, R_h \geq 0$. that are positives. Therefore, the solution will remain in R_+^6 for all $t \geq 0$ with positive initial conditions.

Boundedness of Fractional Model Solution

The total human population from our model is given by;

$N_h(t) = S_h(t) + E_h(t) + I_h(t) + T_h(t) + V_h(t) + R_h(t)$.

So, from our fractional model (16), we now obtain:

$${}_c D_t^{\vartheta} N_h(t) = {}^c D_t^{\vartheta} S_h(t) + {}^c D_t^{\vartheta} E_h(t) + {}^c D_t^{\vartheta} I_h(t) + {}^c D_t^{\vartheta} T_h(t) + {}^c D_t^{\vartheta} V_h(t) + {}^c D_t^{\vartheta} R_h(t).$$

$${}_c D_t^{\vartheta} N_h(t) = \pi - \mu_h N_h(t), \quad (18)$$

Taking the Laplace transformation of (18) we obtained:

$$L\left[{}_c D_t^{\vartheta} N_h(t)\right] = L[\pi - \mu_h N_h(t)],$$

$$S_h^{\varphi} N_h(s) - S_h^{\varphi-1} N_h(0) + \mu_h N_h(s) \leq \frac{\pi}{\mu_h},$$

$$N_h(s) \leq \frac{S_h^{\vartheta-1}}{(S_h^{\vartheta} + \mu)} N_h(0) + \frac{\pi}{s_h(s_h^{\vartheta} + \mu_h)}, \quad (19)$$

By taking the inverse Laplace transform of Eq. (19), we obtained:

$$N_h(t) \leq E_{t\vartheta,1}\left(-\mu_h t^{\vartheta}\right) N_h(0) + \pi E_{t\vartheta,\vartheta+1}\left(-\mu_h t^{\vartheta}\right) \quad (20)$$

At $t \to \infty$, the limit of Eq. (20) becomes:

$$\lim_{t\to\infty} Sup N(t) = \frac{\pi}{\mu_h}.$$

This means that, if $N_{h0} \leq \frac{\pi}{\mu_h}$.

Then, $N_h(t) \leq \frac{\pi}{\mu_h}$which implies that,$N_h(t)$ is bounded.

We now conclude that, this region$\Omega = \Omega_h$, is well posed and equally feasible epidemiologically.

Existence and Uniqueness of our Model Solution

Let the real non-negative be V, we consider $U = [0, V[]$

The set of all continuous function that is defined on P is represented by $N_e^0(V)$ with norm as:

$$\|K\| = Sup\{|K(t)|, t \in V\}.$$

Considering model (14) along with the initial conditions specified, this can be represented as an initial value problem (IVP).

$${}^c D_t^{\vartheta} K(t) = Z(t, K(t)), 0 < t < V < \infty, \quad (21)$$

$K(0) = K_0$.

Where $K(t) = (S_h(t), E_h(t), I_h(t), T_h(t), V_h(t), R_h(t))$. represent the classes and Z be a continuous function defined as follows:

$$Z(t, K(t)) = \begin{pmatrix} Z_1(t, S_h(t)) \\ Z_2(t, E_h(t)) \\ Z_3(t, I_h(t)) \\ Z_4(t, T_h(t)) \\ Z_5(t, V_h(t)) \\ Z_6(t, R_h(t)) \end{pmatrix} = \begin{pmatrix} \pi + \psi_2 V_h - \frac{(\varepsilon_1 I_h + \varepsilon_2 T_h)}{N_h} S_h - (\psi_1 + \mu_h) S_h \\ \frac{(\varepsilon_1 I_h + \varepsilon_2 T_h)}{N_h} S_h - (\theta + \mu_h) E_h \\ \theta E_h - (\phi + \delta + \mu_h) I_h \\ \phi I_h - (\sigma + \alpha\delta + \mu_h) T_h \\ \psi_1 S_h - (\psi_2 + \mu_h) V_h \\ \sigma T_h - \mu_h R_h \end{pmatrix}, \quad (22)$$

Using proposition (2.1), we have that,

$$S_h(t) = S_{h0} + I_t^{\vartheta}\left[\pi + \psi_2 V_h - \frac{(\varepsilon_1 I_h + \varepsilon_2 T_h)}{N_h} S_h - (\psi_1 + \mu_h) S_h\right],$$

$$E_h(t) = E_{h0} + I_t^{\vartheta}\left[\frac{(\varepsilon_1 I_h + \varepsilon_2 T_h)}{N_h} S_h - (\theta + \mu_h) E_h\right], \quad (23)$$

$$I_h(t) = I_{h0} + I_t^{\vartheta}[\theta E_h - (\phi + \delta + \mu_h) I_h],$$

$$T_h(t) = T_{h0} + I_t^{\vartheta}[\phi I_h - (\sigma + \alpha\delta + \mu_h) T_h],$$

$$V_h(t) = V_{h0} + I_t^{\vartheta}[\psi_1 S_h - (\psi_2 + \mu_h) V_h],$$

$$R_h(t) = R_{h0} + I_t^{\vartheta}[\sigma T_h - \mu_h R_h].$$

We now obtained the following:

$$S_{hn}(t) = S_{h0} + \frac{1}{\Gamma(\vartheta)} \int_0^t (t - \lambda)^{\vartheta-1} Z_1\left(\lambda, S_{h(n-1)}(\lambda)\right) d\lambda,$$

$$E_{hn}(t) = E_{h0} + \frac{1}{\Gamma(\vartheta)} \int_0^t (t - \lambda)^{\vartheta-1} Z_2\left(\lambda, E_{h(n-1)}(\lambda)\right) d\lambda,$$

$$I_{hn}(t) = I_{h0} + \frac{1}{\Gamma(\vartheta)}\int_0^t (t-\lambda)^{\vartheta-1} Z_3\left(\lambda, I_{h(n-1)}(\lambda)\right) d\,\lambda,$$
$$T_{hn}(t) = T_{h0} + \frac{1}{\Gamma(\vartheta)}\int_0^t (t-\lambda)^{\vartheta-1} Z_4\left(\lambda, T_{h(n-1)}(\lambda)\right) d\,\lambda, \quad (24)$$
$$V_{hn}(t) = V_{h0} + \frac{1}{\Gamma(\vartheta)}\int_0^t (t-\lambda)^{\vartheta-1} Z_5\left(\lambda, V_{h(n-1)}(\lambda)\right) d\,\lambda,$$
$$R_{hn}(t) = R_{h0} + \frac{1}{\Gamma(\vartheta)}\int_0^t (t-\lambda)^{\vartheta-1} Z_6\left(\lambda, R_{h(n-1)}(\lambda)\right) d\,\lambda.$$

Transforming equation eq. (3.23) to get:

$$X(t) = X(0) + \frac{1}{\Gamma(\vartheta)}\int_0^t (t-\lambda)^{\vartheta-1} Z\left(\lambda, X(\lambda)\right) d\,\lambda. \quad (25)$$

Lemma 1

The Lipchitz condition described from Eq. (25)is satisfied by vector $Z(t, K(t))$ on a set $[0, V[]_+^6]$ with the Lipchitz constant given as:

$\beta = max\big((\varepsilon_1^* + \varepsilon_2^* + \psi_1 + \mu_h), (\theta + \mu_h), (\phi + \delta + \mu_h), (\sigma + \alpha\delta + \mu_h), (\psi_2 + \mu_h), \mu_h\big)$.

Proof.

$\|Z_1(t, S_h) - Z_1(t, S_{h1})\|$

$= \left\|\left(\pi + \psi_2 V_h - \frac{(\varepsilon_1 I_h + \varepsilon_2 T_h)}{N_h} S_h - (\psi_1 + \mu_h) S_h\right) - \pi + \psi_2 V_h - \frac{(\varepsilon_1 I_h + \varepsilon_2 T_h)}{N_h} S_h - (\psi_1 + \mu_h) S_{h1}\right\|,$

$= \left\|\pi + \psi_2 V_h - \frac{(\varepsilon_1 I_h + \varepsilon_2 T_h)}{N_h} S_h - (\psi_1 + \mu_h)\left(S_h - S_{h_1}\right) + \mu_h\left(S_h - S_{h_1}\right)\right\|$

$\leq (\varepsilon_1^* + \varepsilon_2^*)\|S_h - S_{h1}\| + \mu_h\|S_h - S_{h1}\|, \therefore \|Z_1(t, S_h) - Z_1(t, S_{h1})\| \leq (\varepsilon_1^* + \varepsilon_2^* + \psi_1 + \mu_h)\|S_h - S_{h1}\|,$

Similarly, we obtained the following:

$$\left\|Z_2\left(t, \mathrm{E}_h\right) - Z_2\left(t, \mathrm{E}_{h1}\right)\right\| \leq \left(\theta + \mu_h\right)\left\|\mathrm{E}_h - \mathrm{E}_h\right\|,$$
$$\left\|Z_3\left(t, \mathrm{I}_h\right) - Z_3\left(t, \mathrm{I}_h\right)\right\| \leq (\phi + \delta + \mu_h)\left\|\mathrm{I}_h - \mathrm{I}_{h1}\right\|, \quad (26)$$
$$\left\|Z_4\left(t, \mathrm{T}_h\right) - Z_4\left(t, \mathrm{T}_{h1}\right)\right\| \leq (\sigma + \alpha\delta + \mu_h)\left\|T_h - T_{h1}\right\|,$$
$$\left\|Z_5\left(t, \mathrm{V}_h\right) - Z_5\left(t, \mathrm{V}_{h1}\right)\right\| \leq \left(\psi_2 + \mu_h\right)\left\|\mathrm{V}_h - \mathrm{V}_{h1}\right\|,$$

$\|Z_6(t, R_h\quad) - Z_6(t, R_{h1}\quad)\| \leq \mu_h\|R_h - R_{h1}\|.$

Where we obtained:

$\|Z(t, K_1(t)) - Z(t, K_2(t))\| \leq \vartheta\|K_1 - K_2\|,$

$\beta = max\big((\varepsilon_1^* + \varepsilon_2^* + \psi_1 + \mu_h), (\theta + \mu_h), (\phi + \delta + \mu_h), (\sigma + \alpha\delta + \mu_h), (\psi_2 + \mu_h), \mu_h\big).$ (3.26)

Lemma 2

The initial value problem (16), (17) in Eq. (7) exists and will have a unique solution

$K(t) \in D_c^0(E)$.

Using Picard Lindelöfand fixed-point theory, we consider the solution of

$K(t) = S_h\big(K(t)\big)$,

where S is defined as the Picard operator expressed as:

$S_h: D_c^0(E, R_+^6) \to D_c^0(E, R_+^6)$.

Therefore,

$$S_h\big(K(t)\big) = K(0) + \frac{1}{\Gamma(\vartheta)}\int_0^t (t-\lambda)^{\vartheta-1} Z\left(\lambda, K(\lambda)\right) d\,\lambda.$$

which becomes :

$\left\|S_h\big(K_1(t)\big) - S_h\big(K_2(t)\big)\right\|,$

$= \left\|\frac{1}{\Gamma(\vartheta)}\left[\int_0^t (t-\lambda)^{\vartheta-1} Z(\lambda, K_1(\lambda)) - Z(\lambda, K_2(\lambda))\, d\,\lambda\right]\right\|,$

$\leq \frac{1}{\Gamma(\vartheta)}\int_0^t (t-\lambda)^{\vartheta-1}\, \|Z(\lambda, K_1(\lambda)) - Z(\lambda, K_2(\lambda))\, d\,\lambda\|.$

$\leq \frac{\beta}{\Gamma(\vartheta)}\int_0^t (t-\lambda)^{\vartheta-1}\, \|K_1 - K_2\| d\lambda.$

$\left\|S_h\big(K_1(t)\big) - S_h\big(K_2(t)\big)\right\| \leq \frac{\beta}{\Gamma(\vartheta+1)S_h}.$

When $\frac{\beta}{\Gamma(\vartheta+1)} S_h \leq 1$.

Then, the Picard operator gives a contradiction , so Eq.(7) solution is unique.

Fractional Order Model Numerical Results

The generalized fractional Adams–Bashforth–Moulton scheme described by Amos et al. (2024) was used to numerically compute the fractional-order Measles model. The parameter values applied to the system are given in Table 1 where different values of fractional orders are applied and simulated.

Implementation of Fractional Adams–Bashforth–Moulton Method

Amos et al. (2024)), Atokolo et al. (2024) and Abah et al. (2024) approach is used in this study. The fractional Adams–Bashforth–Moulton scheme is used to find an approximate solution to the fractional Measles model in equation (7). Therefore, the fractional model of (7) is re-written as:

$$ {}^{c}D_t^{\vartheta} P(t) = Q(t, q(t)), 0 < t < \beta, \quad (27)$$

$$P^{(n)}(0) = P_0^{(n)}, n = 1,0,\dots, q, q = [\vartheta].$$

Where $P = (S_h^*, E_h^*, I_h^*, T_h^*, V_h^*, R_h^*) \in R_+^6$ and $V(t, q(t))$ is a real valued function that is continuous.

Eq. (27) can therefore be represented using the concept of fractional integral as follows:

$$P(t) = \sum_{n=0}^{m-1} P_0^{(n)} \frac{t^n}{n!} + \frac{1}{\Gamma(\vartheta)} \int_0^t (t-y)^{\vartheta-1} R\big(k, m(k)\big) dk \quad (28)$$

Using the method described in Amos et al. (2024), we let the step size $g = \frac{\beta}{N}, N \in N$ with a grid that is uniform on $[0, \beta]$. Where $t_c = cr, c = 0,1,1,\dots N$. Therefore, the fractional order model of Measles model presented in (7) can be approximated as :

$$S_{h(k+1)}(t) = S_{h0} + \frac{g^{\vartheta}}{\Gamma(\vartheta+2)}\left\{\pi + \psi_2 V_h^n - \frac{(\varepsilon_1 I_h^n + \varepsilon_2 T_h^n)}{N_h^n} S_h^n - (\psi_1 + \mu_h) S_h^n\right\} +$$

$$\frac{g^{\vartheta}}{\Gamma(\vartheta+2)} \sum_{y=0}^{k} dy, k+1 \left\{\pi + \psi_2 V_{hy} - \frac{(\varepsilon_1 I_{hy} + \varepsilon_2 T_{hy})}{N_{hy}} S_{hy} - (\psi_1 + \mu_h) S_{hy}\right\},$$

$$E_{h(k+1)}(t) = E_{h0} + \frac{g^{\vartheta}}{\Gamma(\vartheta+2)}\left\{\frac{(\varepsilon_1 I_h^n + \varepsilon_2 T_h^n)}{N_h^n} S_h^n - (\theta + \mu_h) E_h^n\right\} +$$

$$\frac{g^{\vartheta}}{\Gamma(\vartheta+2)} \sum_{y=0}^{k} dy, k+1 \left\{\frac{(\varepsilon_1 I_{hy} + \varepsilon_2 T_{hy})}{N_{hy}} S_{hy} - (\theta + \mu_h) E_{hy}\right\},$$

$$I_{h(k+1)}(t) = I_{h0} + \frac{g^{\vartheta}}{\Gamma(\vartheta+2)}\{\theta E_h^n - (\phi + \delta + \mu_h) I_h^n\} +$$

$$\frac{g^{\vartheta}}{\Gamma(\vartheta+2)} \sum_{y=0}^{k} dy, k+1\{\theta E_{hy} - (\phi + \delta + \mu_h) I_{hy}\}, \quad (29)$$

$$T_{h(k+1)}(t) = T_{h0} + \frac{g^{\vartheta}}{\Gamma(\vartheta+2)}\{\phi I_h^n - (\sigma + \alpha\delta + \mu_h) T_h^n\} +$$

$$\frac{g^{\vartheta}}{\Gamma(\vartheta+2)} \sum_{y=0}^{k} dy, k+1\{\phi I_{hy} - (\sigma + \alpha\delta + \mu_h) T_{hy}\},$$

$$V_{h(k+1)}(t) = V_{h0} + \frac{g^{\vartheta}}{\Gamma(\vartheta+2)}\{\psi_1 S_h^n - (\psi_2 + \mu_h) V_h^n\} +$$

$$\frac{g^{\vartheta}}{\Gamma(\vartheta+2)} \sum_{y=0}^{k} dy, k+1\{\psi_1 S_{hy} - (\psi_2 + \mu_h) V_{hy}\},$$

$$R_{h(k+1)}(t) = R_{h0} + \frac{g^{\vartheta}}{\Gamma(\vartheta+2)}\{\sigma T_h - \mu_h R_h^n\} +$$

$$\frac{g^{\vartheta}}{\Gamma(\vartheta+2)} \sum_{y=0}^{k} dy, k+1\{\sigma T_{hy} - \mu_h R_{hy}\}.$$

Where

$$S_{h(k+1)}^n(t) = S_{h0} + \frac{1}{\Gamma(\vartheta)} \sum_{y=0}^{k} f_{y,k+1} \left\{\pi + \psi_2 V_{hy} - \frac{(\varepsilon_1 I_{hy} + \varepsilon_2 T_{hy})}{N_{hy}} S_{hy} - (\psi_1 + \mu_h) S_{hy}\right\},$$

$$E_{h(k+1)}^n(t) = E_{h0} + \frac{1}{\Gamma(\vartheta)} \sum_{y=0}^{k} f_{y,k+1} \left\{\frac{(\varepsilon_1 I_{hy} + \varepsilon_2 T_{hy})}{N_{hy}} S_{hy} - (\theta + \mu_h) E_{hy}\right\},$$

$$I_{h(k+1)}^n(t) = I_{h0} + \frac{1}{\Gamma(\vartheta)} \sum_{y=0}^{k} f_{y,k+1} \{\theta E_{hy} - (\phi + \delta + \mu_h) I_{hy}\},$$

$$T_{h(k+1)}^n(t) = T_{h0} + \frac{1}{\Gamma(\vartheta)} \sum_{y=0}^{k} f_{y,k+1} \{\phi I_{hy} - (\sigma + \alpha\delta + \mu_h) T_{hy}\}, \quad (30)$$

$$V_{h(k+1)}^n(t) = V_{h0} + \frac{1}{\Gamma(\vartheta)} \sum_{y=0}^{k} f_{y,k+1} \{\psi_1 S_{hy} - (\psi_2 + \mu_h) V_{hy}\},$$

$$R_{h(k+1)}^n(t) = R_{h0} + \frac{1}{\Gamma(\vartheta)} \sum_{y=0}^{k} f_{y,k+1} \{\sigma T_{hy} - \mu_h R_{hy}\}.$$

From (29) and (30) obtained:

$dy_{,K+1} = K^{\vartheta+1} - (k-\vartheta)(k+\vartheta)^{\vartheta}, y = 0,$

$(k-y+2)^{\vartheta+1} + (k-\vartheta)^{\vartheta+1} - 2(k-y+1)^{\vartheta+1}, 1 \le y \le k,$

and $f_{y,k+1} = \frac{g^{\vartheta}}{\vartheta}\left[(k-y+1)^{\vartheta}(k-y)^{\vartheta}\right], 0 \le y \le k.$

Importance of using the Fractional Adam-Bashforth Moulton Method in obtaining the Numerical Solutions of the Model

i. The fractional Adams–Bashforth–Moulton method is high-order with one extra function evaluation per step.
ii. It has an internal error control, and is widely used in integrated solvers for ordinary differential equations.
iii. This approach is a practical tool for the numerical solution of partial and fractional-order differential equations since it has been successfully used in various disciplines such as engineering, chemistry, and medicine.

Fractional Order Measles Model Simulation

In this section, we present the numerical simulation of the Measles model using the three differential operators used. The values of the model variables (parameters) used in this simulation are given in Table 2. The parameters are cited from sources in APA format.

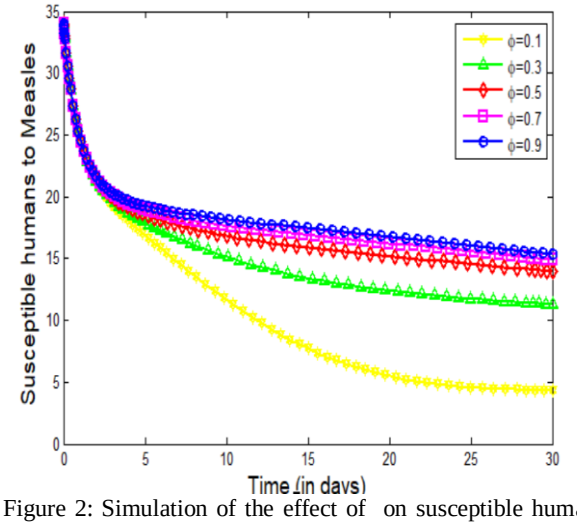

Figure 2: Simulation of the effect of on susceptible human population

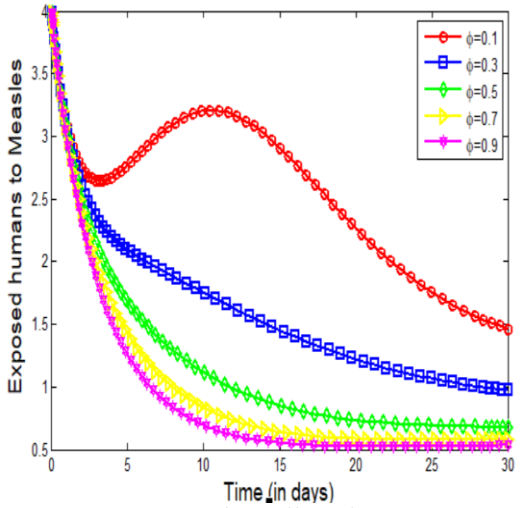

Figure 3: Simulation of the effect of on exposed human population

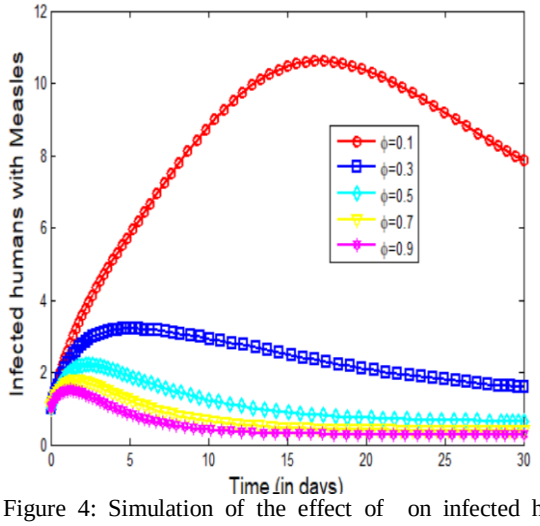

Figure 4: Simulation of the effect of on infected human population

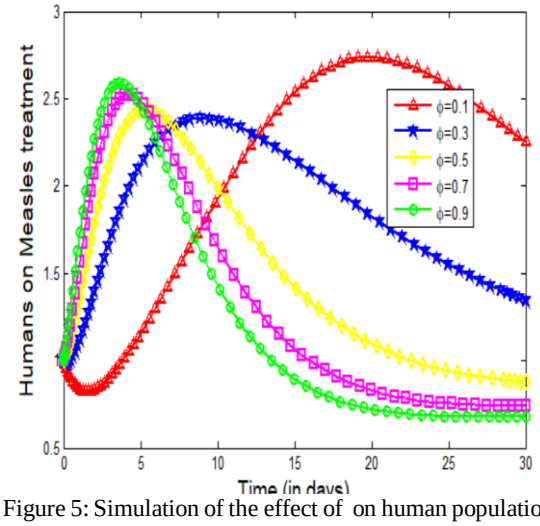

Figure 5: Simulation of the effect of on human population on treatment

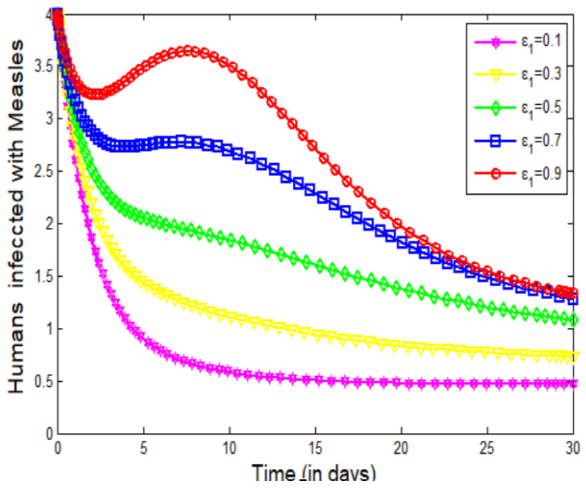

Figure 6: Simulation of the effect of ψ_1 on exposed human population

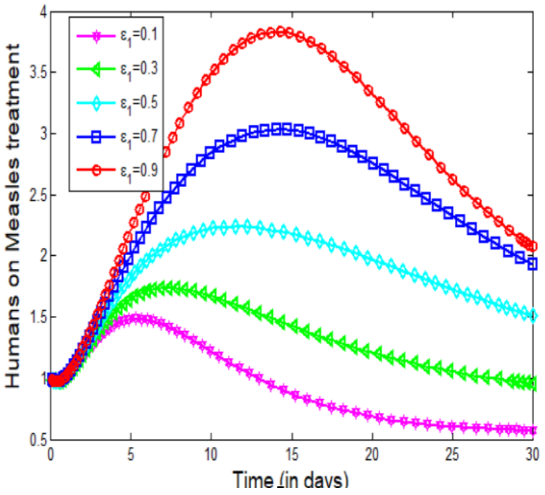

Figure 7: Simulation of the effect of ψ_1 on infected human population

Numerical Simulations

Figure (4.1) shows the simulation of the effect of the treatment rate ϕ on the susceptible human population to measles disease. It is seen that with the increase in ϕ, the susceptible population increases a lot with time. Figure (4.2) presents the simulation of the effect of the treatment rate ϕ on the population of exposed humans with measles disease. It is observed that with increasing ϕ, the exposed population decreases considerably with time. Figure (4.3) shows the simulation of the effect of the treatment rate ϕ on the infected human population with measles disease. It is seen that as ϕ increases, the infected population decreases drastically over time. Figure (4.4) shows simulation of the effect of the treatment rate ϕ on human population on measles treatment rate. As ϕ increases, human population on treatment increases significantly with time. Figure (4.5) is a simulation of the effect of the contact rate ε_1 on the infected human population with measles disease. It is observed that for ε_1 increase in time, infected population increases significantly with increase in ε_1. Figure (4.6) shows the simulation of the impact of the contact rate ε_1 on human population for measles treatment. It is observed that with the increase of ε_1, human population on treatment increases significantly with time.

Table 2: Table of Parameter Values and their Sources

Parameter	Baseline Value	Source
π	0.45	Hall et al. (2022).
μ_h	0.000039	(WHO, 2023)
ω	0.65	Hall et al. (2022).
θ	0.1429	Anderson and May (1991)
ϕ	0.35	Hall, et al. (2022).
σ	0.75	CDC (2022)
δ	0.015	WHO (2023)
α	0.60	Assumed
ψ_1	0.50	Feldman et al. (2021).
ψ_2	0.02	Feldman et al. (2021).

CONCLUSION

In this study, a fractional-order mathematical model of the transmission dynamics of Measles disease has been developed and analyzed by including the treatment, vaccination, and contact rates as some of the important epidemiological parameters. Existence and uniqueness analysis of the model showed that the model was well-posed and stability analysis showed that the conditions for disease persistence and eradication were governed by the basic reproduction number. The outcomes indicated that bringing treatment and vaccination rates up to a high level significantly decreased disease transmission and could bring down the basic reproduction number under one, which is a prerequisite for a successful disease control. On the other hand, increased contact rates lead to more disease transmission and maintenance in the population. The numerical simulations with the fractional Adams–Bashforth–Moulton scheme also showed that better treatment and vaccination strategies resulted in greater reduction in exposed and infected populations while greater contact rate resulted in greater number of infected and treatment needed. Overall, the results show the need for an integrated control strategy of effective treatment, high vaccination coverage, and control of contact transmission, to control and ultimately eradicate Measles disease.

REFERENCES

Abah E., Bolaji B., Atokolo W., Amos J., Acheneje G.O., Omede B.I, Amos J.,Omeje D. (2024), Fractional mathematical model for the Transmission Dynamics and

control of Diphtheria ,International Journal of mathematical Analysis and Modelling,Vol.7,ISSN:2682-5694.

Abro K., A. Atangana, J.F. Gómez-Aguilar, (2021) An analytic study of bio heat transfer Pennes model via modern non-integers differential techniques, Eur. Phys. J. Plus 136 http://dx.doi.org/10.1140/epjp/s13360-021-02136-x

Agahiu, N., Bolaji B., Acheneje, G. O., & Atokolo W (2024). Approximate solution of fractional order mathematical model on the co-transmission of Zika and Chikungunya virus using Laplace-Adomian decomposition Method. Int. J. Mathematics. 07(03), 47-81.

Ahmed, I., Goufo, E.F.D., Yusuf, A., Kumam, P., Chaipanya, P., & Nonlaopon, K. (2021). "An epidemic prediction from analysis of a combined HIV-COVID-19 co-infection model via ABC fractional operator." *Alexandria Engineering Journal*, 60(3), pp. 2979–2995.

Ali Z., Zada A., Shah K., (2017) Existence and stability analysis of three point boundary value problem, Int. J. Appl. Comput. Math. 3 651–664, http://dx.doi.org/10.1007/s40819-017-0375-8

Ameh, P.O., Omede, B.I, & Bolaji.B. (2020). Dynamical analysis of a two strain treatment model for Anthrax in a population where it is deployed as bio-terrorism weapon. Journal of the Nigerian Society for Mathematical Biology. Volume 3, pp. 34 – 77.

Amos, J., Omale, D., Atokolo, W., Abah, E. Omede, B. I., Acheneje, G. O., Bolaji, B. (2024). Fractional mathematical model for the Transmission Dynamics and control of Hepatitis C,FUDMA Journal of Sciences,Vol.8,No.5,pp.451-463, DOI: https://doi.org/10.33003/fjs-2024-0805-2883

Atokolo, W., Aja, R. O., Aniaku, S. E., Onah, I. S., & Mbah, G.C. (2022). "Approximate solution of the fractional order sterile insect technology model via the Laplace-Adomian Decomposition Method for the spread of Zika virus disease," *International Journal of Mathematics and Mathematical Sciences*, 2022(1), Article 2297630.

Atokolo, W.A., Remigius Aja, O., Omale, D., Ahman, Q. O., Acheneje, G.O., Amos, J. (2024). "Fractional mathematical model for the transmission dynamics and control of Lassa fever," *Journal of Fractional Calculus and Applied Mathematics*, 2773-1863, DOI: https://doi.org/10.1016/j.fraope.2024.100110

Atokolo, W.A., Remigius Aja, O., Omale, D., Paul, R.V., Amos, J., Ocha, S.O. (2023), "Mathematical modeling of the spread of vector-borne diseases with influence of vertical transmission and preventive strategies," *FUDMA Journal of Sciences*, Vol. 7, No. 6 (Special Issue), pp. 75–91, DOI: https://doi.org/10.33003/fjs-2023-0706-2174

Baskonus. H.M., Bulut H., (2015) On the numerical solutions of some fractional ordinary differential equations by fractional Adams Bashforth-Moulton Method, Open Math. 13 1.

Bolaji B., Ani F., Omede, B. I, Acheneje, G. O, Ibrahim A. (2024). A model for the control of transmission dynamics of human Monkeypox disease in sub-Saharan Africa. J. Nig. Soc. Phys. Sci. 6 1800. Available online at: https://journal.nsps.org.ng/index.php/jnsps - Scopus indexed Journal

Bolaji, B, Odionyenma U. B., Omede B. I., Ojih, P., and Abdullahi, B., Ibrahim, A. (2023). Modelling the transmission dynamics of Omicron variant of COVID-19 in densely populated city of Lagos in Nigeria, J. Nig. Soc. Phys. Sci. 5 1055. Available online at: https://journal.nsps.org.ng/index.php/jnsps - Scopus indexed Journal.

Chen, Y., Wong, K., & Zhao, L. (2023). "Modeling the impact of vaccination strategies on hepatitis C and COVID-19 coinfection dynamics." *Journal of Vaccine*, 41(15), pp. 2897–2905.

Chikaki, E., Ishikawa, H. (2009), "A Dengue transmission model in Thailand considering sequential infections with all four serotypes," *J. Infect. Dev. Ctries.*, 3(9), pp. 711–722.

Das, R., Patel, S., & Kumar, A. (2024), "Mathematical modeling of hepatitis C and COVID-19 coinfection in low- and middle-income countries: challenges and opportunities," *BMC Public Health*, 24(1), pp. 587.

Diethelm, K. (1999). The Frac PECE subroutine for the numerical solution of differential equations of fractional order.

Jalija .E., Amos .J., Atokolo ,W., Omale .D.Abah . U.Alih.U., P.A.Alabi, and BolajiB. (2025) Numerical investigations on Dengue fever model through singular and non-singular fractional operators. International Journal of Mathematical Analysis and Modelling (2025) 8(1):216-242

Emmanuel, L., Omale, D., Atokolo, W., Amos, J., Abah, E., Ojonimi, A., Onoja, T., Acheneje, G., & Bolaji, B. (2025). Fractional mathematical model for the dynamics of pneumonia transmission with control using fixed point theory. *GPH-International Journal of Mathematics*, 8(5), 55-86. https://doi.org/10.5281/zenodo.16364036

Jalija .E., Amos .J., Atokolo ,W., Abah .E., Agbata B.C.,Acheneje G.O, Shyamsunder, Bolarinwa Bolaji (2025), Numerical solution of fractional order typhoid fever model via the generalized fractional Adams-Bashforth-Moulton approach. Network Modeling Analysis in Health Informatics and Bioinformatics (2026) 15:68 https://doi.org/10.1007/s13721-026-00743-1

Odiba P. O, Acheneje, G. O, Bolaji B. (2024). A compartmental deterministic epidemiological model with non-linear differential equations for analysing the co-infection dynamics between COVID-19, HIV, and Monkeypox diseases. Healthcare Analytics, 5 100311. Available online at: https://doi.org/10.1016/j.health.2024.100311Journal

Ojonimi A.A., Amos J., Atokolo W., Omale D., Emmanuel L.M., Abah E., Acheneje G.O., Bolaji B. Numerical solution of fractional order Hepatitis B model via the generalized fractional Adams–Bashforth–Moulton approach. Journal of Science Research and Reviews 2(5) (2025) 33–48. https://doi.org/10.70882/josrar.2025.v2i5.119

Omale, D., Atokolo, W., .Akpa, M., (2020). Global stability and sensitivity analysis of transmission dynamics of tuberculosis and its control, A case study of Ika general

hospital Ankpa, Kogi State, Nigeria. Acad. J. Stat. Math. 6, 5730-7151.

Omale, D., Ojih, P., Atokolo, W., Omale, A., Bolaji.B. (2021), Mathematical model for transmission dynamics of HIV and Tuberculosis co-infection in Kogi State, Nigeria. Journal of Mathematical Computational Science. 11, No. 5, 5580-5613. Available online at: https://doi.org/10.28919/jmcs/6080

Omame, A.M., Abbas, M., Onyenegecha, C.P. (2022), "A fractional order model for the co-interaction of COVID-19 and hepatitis B virus." *Journal of Mathematical Biology*, pp. 112–118.

Omede, B. I., Bolarinwa Bolaji, Olumuyiwa, P. J., Ibrahim, A. A. and Oguntolu F. A (2023). Mathematical analysis on the vertical and horizontal transmission dynamics of HIV and Zika virus co-infection. Franklin open 6 100064. https://doi.org/10.1016/j.fraope.2023.100064 - Elsevier Journal (Scopus indexed)

Omede, B. I., Olumuyiwa, P. J., Atokolo, W., Bolaji, B. & Ayoola, T. A. (2023). A mathematical analysis of the two-strain tuberculosis model dynamics with exogenous re-infection. Healthcare Analytics 4, 100266. https://doi.org/10.1016/j.health.2023.100266 - Scopus indexed Journal

Omede, B.I., Israel, M., Mustapha, M. K., Amos, J., Atokolo, W., & Oguntolu, F. A. (2024). "Approximate solution to the fractional soil-transmitted helminth infection model using Laplace-Adomian Decomposition Method," *International Journal of Mathematics*, 07(04), pp. 16–40.

Omonu, G. U., Ameh, P.O., Omede, B.I, & Bolaji.B (2019), Mathematical modelling of Tuta Absoluta on Tomato plants. Journal of the Nigerian Society for Mathematical Biology. 2(1): 14-31.

Philip J., Omale D., Atokolo W., Amos J., Acheneje G.O., Bolaji B. (2024), Fractional mathematical model for the Transmission Dynamics and control of HIV/AIDs,FUDMA Journal of Sciences,Vol.8,No.6,pp.451-463, DOI: https://doi.org/10.33003/fjs-2024-0805-2883

Smith, J., Johnson, A.B., & Lee, C. (2023), "Modeling the coinfection dynamics of hepatitis C and COVID-19: A systematic review," *Journal of Epidemiology and Infection*, 151(7), pp. 1350–1365.

Udoka, B. O., Nometa, I. & Bolaji, B. (2023). Analysis of a model to control the co-dynamics of Chlamydia and Gonorrhea using Caputo fractional derivative. Mathematical Modelling and Numerical Simulation with Applications, 2023, 3(2), 111–140. Available online at: https://doi.org/10.53391/mmnsa.1320175 - Scopus indexed Journal.

Ullah, A. Abdeljawad Z., Hammouch T. Z., Shah K. (2020). "A hybrid method for solving fuzzy Volterra integral equations of separable type kernels," *Journal of King Saud University - Science*, 33, DOI: https://doi.org/10.1016/j.jksus.2020.101246

Yunus, A.O, M.O. Olayiwola, M.A. Omolaye, A.O. Oladapo, (2023). A fractional order model of lassa fever disease using the Laplace-Adomian decomposition method, Health Care Anal. 3 100167, www.elsevier.com/locate/health Health Care Analytics.

Zhang, R. M. Li, (2022) bilinear residual network method for solving the exactly explicit solutions of nonlinear evolution equations, Nonlinear Dynam. 108 http://dx.doi.org/10.1007/s11071-022-07207-x

Zhang, R.F., Li, M.-C., J.Y. Gan, Q. Li, Z.-Z. Lan, (2022). Novel trial functions and rogue waves of generalized breaking soliton equation via bilinear neural network method, Chaos Solitons Fractals 154